Available online at www.sciencedirect.com

SCIENCE DIRECT®

Thin Solid Films 480–481 (2005) 426–432

www.elsevier.com/locate/tsf

# $Cu_2ZnSnS_4$ thin film solar cells

Hironori Katagiri

*Nagaoka National College of Technology, 888 Nishikatakai, Nagaoka, Niigata 940-8532, Japan*

Available online 10 March 2005

**Abstract**

Aiming to develop the solar cells free from the environmental contaminants, promising solar cell of a thin film type could be produced by using $Cu_2ZnSnS_4$ (CZTS) film as the absorber. The CZTS film possesses promising characteristic optical properties; band gap energy of about 1.5 eV and large absorption coefficient in the order of $10^4$ $cm^{-1}$, which means large possibility of commercial production of the most suitable absorber by using the CZTS film. In addition, as the CZTS film contains neither rare metals nor toxic materials, combining this film with Cd-free buffer layer, we can expect coming solar cells with nontoxic thin films in the near future.

CZTS thin films were able to be produced successfully in our previous work by vapor phase sulfurization of the stacked precursors that were prepared by sequential vacuum evaporation of Cu, Sn, and ZnS. The best conversion efficiency with the heterojunction of ZnO:Al/CdS and CZTS was 5.45%, which showed the possibility of a very low cost solar cell. It has been, however, quite difficult to prepare CZTS film with high reproducibility.

This paper showed the photovoltaic properties of CZTS-based thin film solar cells fabricated by using three types of precursors: (1) the conventional precursor with stacked layers of Cu/Sn/ZnS, (2) the modified precursor with the stacking order of Sn/Cu/ZnS, and (3) the precursor with five periods of $Cu/SnS_2/ZnS$, which was produced to increase the amount of S and to enhance the interdiffusion in precursor.


*Keywords:* *I*; Deposition process; Photovoltage; Solar cells

## 1. Introduction

$Cu_2ZnSnS_4$ (CZTS), which consists of abundant materials, is a new type of an absorber for thin film solar cells. This semiconductor film can be obtained by replacing half of the indium atoms in chalcopyrite $CuInS_2$ with zinc, and by replacing the other half with tin. The abundance of zinc, tin, and indium in the crust of the earth is 75, 2.2, and 0.049 ppm, respectively [1]. All constituents in this CZTS film are abundant in the crust of the earth, and are nontoxic. In 1988, Ito and Nakazawa reported, for the first time, the photovoltaic effect in the heterodiode that consists of cadmium-tin-oxide transparent conductive film and CZTS thin film on a stainless steel substrate. They reported the open-circuit voltage as 165 mV [2]. In 1989, by annealing the same device in air, they achieved the open-circuit voltage of 250 mV and the short-circuit current of 0.1 $mA/cm^2$ [3]. In 1997, Friedlmeier et al. fabricated CZTS thin films by thermal evaporation of the elements and binary chalcogenides in high vacuum. For the heterojunction of this film and the CdS/ZnO window layer, they reported the highest conversion efficiency of 2.3% and the highest open-circuit voltage of 570 mV [4]. In 2003, Seol et al. prepared CZTS thin films by RF magnetron sputtering. They reported that the refractive index was 2.07, the absorption coefficient was about $10^4$ $cm^{-1}$, and that the band gap energy was about 1.51 eV [5].

In 1996 at PVSEC-9 we reported, for the first time, that CZTS thin films are able to be formed successfully by vapor phase sulfurization of E–B-evaporated precursors; and the conversion efficiency is 0.66% with the device structure of ZnO:Al/CdS/CZTS/Mo/soda lime glass (SLG) substrate [6]. In 1999, the conversion efficiency was increased up to 2.63%, which was reported at PVSEC-11 [7]. Furthermore, we attained the highest conversion efficiency of 5.45% in 2003, which was reported at WCPEC-3 [8].

0040-6090/$ - see front matter © 2004 Elsevier B.V. All rights reserved.
doi:10.1016/j.tsf.2004.11.024

Table 1
Thickness of each layer and predicted atomic ratio in the precursor of Type-PA[a]

| Precursor name | Thickness of each layer (nm) | | | Predicted atomic ratio | |
|---|---|---|---|---|---|
| | ZnS | Sn | Cu | Cu/(Zn+Sn) | Zn/Sn |
| PA90 | 330 | 150 | 90 | 0.55 | 1.51 |
| PA100 | 330 | 150 | 100 | 0.61 | 1.51 |
| PA110 | 330 | 150 | 110 | 0.67 | 1.51 |
| PA120 | 330 | 150 | 120 | 0.73 | 1.51 |
| PA130 | 330 | 150 | 130 | 0.79 | 1.51 |

[a] Different types of precursors.

The present paper reports the results of our investigation on CZTS-based thin film solar cells with three types of precursors.

## 2. Experimental

### 2.1. Sample preparation

Fabrication method of CZTS thin films, which have been used in our laboratory, is vapor phase sulfurization. This method consists of two-stage process of the fabrication of precursor with vacuum deposition technique followed by the sulfurization within the atmosphere of $N_2$+$H_2S$ (5%). This method will be one of the most useful processes for a large-scale solar cell production.

In this study, two types of vacuum deposition system were used to prepare three types of precursors: (1) Electron-beam evaporation system with the planetary mechanism. Eighteen precursors with the same composition are prepared at the same time. By using those precursors, we can examine the following sulfurization condition in detail. (2) Electron-beam evaporation system with elevated substrate temperature up to 400 °C. By post-annealing in high vacuum, the interdiffusion of each stacked layer of precursor can be increased.

In order to synthesize CZTS films, the precursors were sulfurized by the heat treatment in the atmosphere of $N_2$+$H_2S$ (5%). This sulfurization system consists of the stainless steel chamber and the turbo molecular pump (TMP). The precursors were heated by an infrared lamp located outside of the chamber through the quarts window in this study.

The heterojunction in the final solar cell consists of chemical-bath-deposited (CBD) CdS and sputtered ZnO:Al on CZTS films that were fabricated on a Mo-coated SLG substrate. $CdI_2$ was used as the Cd-source of CBD solution, and ZnO:$Al_2O_3$ (2 wt.%) was used as the target in the sputtering system.

### 2.2. Characterization

Scanning Electron Microscope (SEM) was used to examine both the film morphology and the film thickness. The chemical composition was determined by Energy Dispersive Spectrometry (EDS). Solar simulator was used for the measurement of the conversion efficiency; illuminated *I–V* characteristics of the solar cell. The system used in this measurement was WACOM WXS-50C-1.5 and Keithley 2400. Optel ND-110A; photo spectrometer with a constant energy was used for the measurement of the quantum efficiency (QE). Agilent 4284A; precision LCR meter was used for the measurement of the *C–V* characteristics.

## 3. Results and discussion

### 3.1. Cu/Sn/ZnS precursor

By using electron-beam evaporation technique, Cu/Sn/ZnS stacked layers were fabricated on the Mo-coated SLG substrates heated to 150 °C. By the deposition of ZnS the first and Sn the next then Cu the last, these stacked precursors on the substrates were prepared. In this study, both thicknesses of ZnS and Sn were set constant as 330 and 150 nm, respectively. Only the thickness of Cu was varied from 90 nm to 130 nm. These precursors were named as PA90 to PA130, corresponding to the thickness of Cu. Table 1 shows the thickness of each layer of precursors and the composition ratio of each element predicted by their density and atomic weight. For suppressing the deviation of the resulted compositions from that of the precursors through the sulfurization period, we increased the composition ratio of Zn/Sn over stoichiometry in the precursor fabrication stage.

These precursors were sulfurized in the atmosphere of $N_2$+$H_2S$ (5%) to fabricate the CZTS thin films. The sulfurization system is almost the same as that reported previously with the exception of a heating apparatus. In this study, the precursors were heated by an infrared lamp

Table 2
Chemical compositions of CZTS films of Type-A

| CZTS name | Chemical compositions (at.%) | | | | Ratio of composition | | |
|---|---|---|---|---|---|---|---|
| | Cu | Zn | Sn | S | Cu/(Zn+Sn) | Zn/Sn | S/Metal |
| CZTS-A90 | 18 | 13 | 15 | 55 | 0.66 | 0.88 | 1.20 |
| CZTS-A100 | 20 | 13 | 14 | 54 | 0.75 | 0.91 | 1.17 |
| CZTS-A110 | 21 | 13 | 11 | 55 | 0.85 | 1.19 | 1.24 |
| CZTS-A120 | 21 | 13 | 12 | 54 | 0.84 | 1.16 | 1.17 |
| CZTS-A130 | 22 | 12 | 12 | 53 | 0.90 | 0.99 | 1.15 |

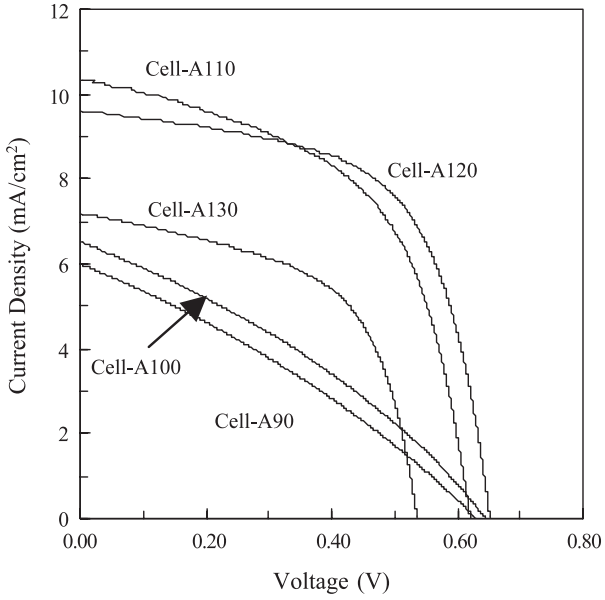


Fig. 1. Illuminated *I–V* characteristics of cells A90 to A130. These numbers correspond to the thickness of Cu in those precursors.

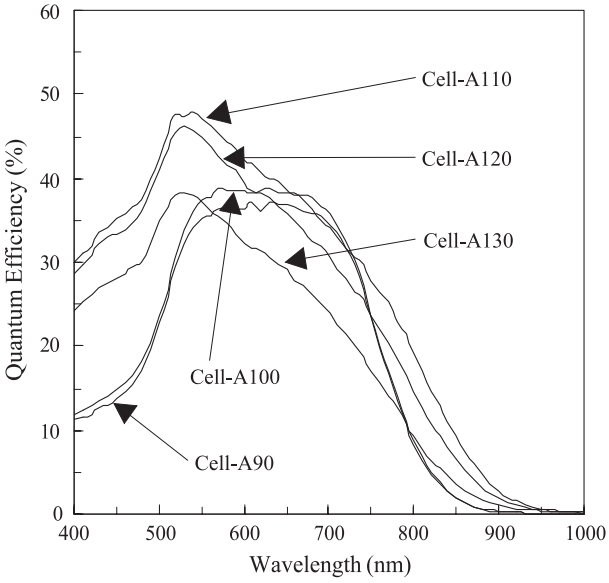


Fig. 2. Quantum efficiency curves of cells A90 to A130.

located outside of the chamber through the quarts window. The temperature was raised up to 200 °C at the rate of 10 °C/min, and to 550 °C at the rate of 2 °C/min finally. The final temperature was maintained at 550 °C for 3 h, and the reactive gas was replaced by $N_2$ thereafter. After the sulfurization, the furnace was cooled to 300 °C at the rate of 2 °C/min, and then cooled naturally to the room temperature. Resulted CZTS thin films were named as CZTS-A90 to A130 corresponding to the name of each precursor.

Table 2 shows the chemical compositions of CZTS-A. From Tables 1 and 2, it is evident that the ratio of Zn/Sn in all films decreases after the sulfurization from 1.51 to that of nearly stoichiometry, while the ratio of Cu/(Zn+Sn) increases. It was confirmed that the sufficient sulfurization was performed in this study, because the ratio of S/Metal increases from 0.48 to 1.15 through the sulfurization.

Fig. 1 shows the *I–V* characteristics of CZTS-based thin film solar cells; Cell-A90 to A130. Table 3 shows the photovoltaic properties obtained from the *I–V* characteristics. The Cell-A120, the Cu thickness is 120 nm and the active area is 0.129 $cm^2$, showed the open-circuit voltage of 652 mV, the short-circuit current of 9.60 $mA/cm^2$, the fill factor (FF) of 0.61, and the conversion efficiency of 3.80%. Both the Cell-A90 and A100 showed the open-circuit voltage of over 620 mV. They showed, however, the low short-circuit current of under 7.00 $mA/cm^2$ and the small fill factor of about 0.30. Fig. 2 shows the quantum efficiency (QE) of Cell-A. In Fig. 2, it is confirmed that the QE of both Cell-A90 and A100 are quite degraded in the range of wavelength under 500 nm. These absorber layers possess the ratio of Cu/(Zn+Sn) of under 0.75 that is too lower than the stoichiometry. For the Cell-A130, the fill factor and the configuration of QE spectrum were nearly the same as those of Cell-A120. The open-circuit voltage was, however, quite low such as 536 mV. The ratio of Cu/(Zn+Sn) of Cell-A130 was 0.90, while those of other cells were under 0.85. It should be noted here that two cells exhibited the higher conversion efficiency; Cell-A110 and A120 possess the ratio of Cu/(Zn+Sn) of around 0.85. In the series of Cell-A, the short-circuit current increases with the increase in the ratio of Zn/Sn.

Fig. 3 shows the SEM micrograph of CZTS absorber used in Cell-A120. We can see that the surface is quite rough and there are many voids. Fig. 4 shows the SEM micrograph of the precursor of PA120 used in CZTS-A120. We can see many voids unexpectedly at the stage of precursor fabrication. From these results of SEM observation, it was confirmed that the surface morphology of CZTS film is considerably affected by that of precursor.

Table 3
Photovoltaic properties of cells of Type-A

| Cell name | Cu (nm) | Area ($cm^2$) | Voc (mV) | Isc ($mA/cm^2$) | Efficiency (%) | FF | Rs (Ω) | Rsh (Ω) |
|---|---|---|---|---|---|---|---|---|
| Cell-A90 | 90 | 0.116 | 629 | 5.99 | 1.17 | 0.31 | 60.3 | 170 |
| Cell-A100 | 100 | 0.121 | 646 | 6.54 | 1.38 | 0.33 | 43.8 | 197 |
| Cell-A110 | 110 | 0.123 | 621 | 10.33 | 3.50 | 0.55 | 8.7 | 302 |
| Cell-A120 | 120 | 0.129 | 652 | 9.60 | 3.80 | 0.61 | 7.7 | 544 |
| Cell-A130 | 130 | 0.099 | 536 | 7.17 | 2.17 | 0.56 | 8.3 | 304 |

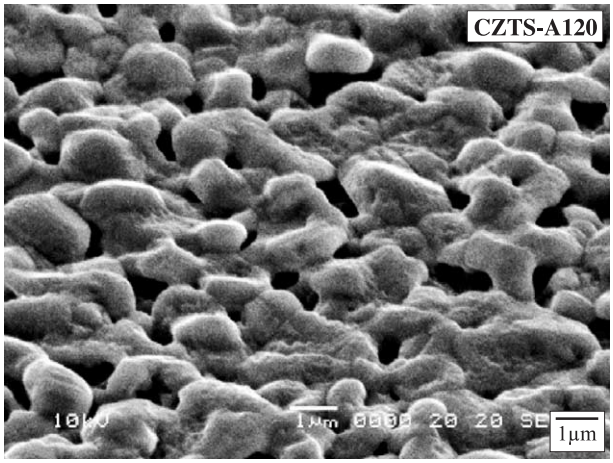


Fig. 3. SEM micrograph of the surface of CZTS-A120 using the conventional Cu/Sn/ZnS precursor.

### 3.2. Sn/Cu/ZnS precursor

In order to improve the surface morphology of the precursor, the stacking order was examined. Fig. 5 shows the SEM micrograph of the surface of the stacked layer of

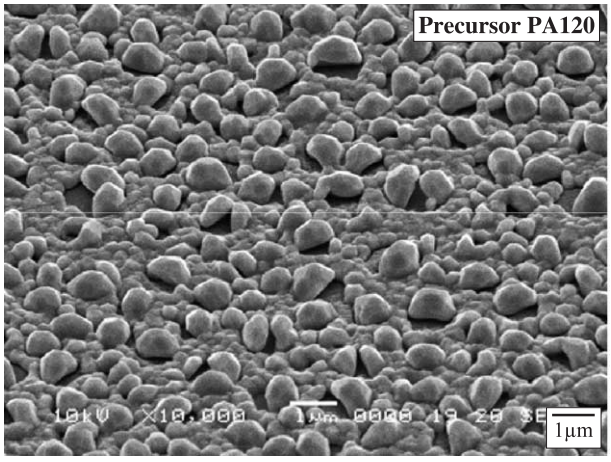


Fig. 4. SEM micrograph of the surface of precursor PA120.

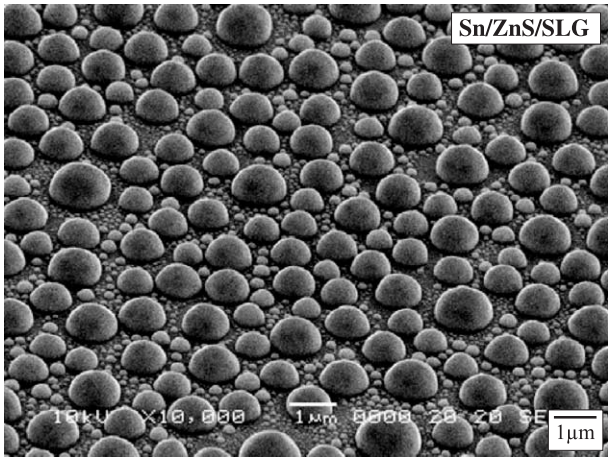


Fig. 5. SEM micrograph of the stacked layer of Sn/ZnS/SLG.

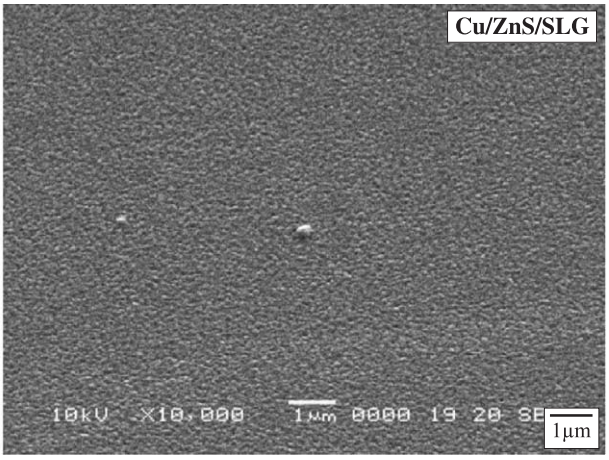


Fig. 6. SEM micrograph of the stacked layer of Cu/ZnS/SLG.

Sn/ZnS/SLG. We can see the hemispheroid of Sn on the very smooth surface of ZnS. Fig. 6 shows the SEM micrograph of the surface of the stacked layer of Cu/ZnS/SLG. In this figure, we can see that the surface of stacked layer with new order is quite smooth. From the results of these preliminary examinations, we fabricated the new type of precursors of Sn/Cu/ZnS stacked layers and named them as precursor of Type-PB. The thickness of each layer was as follows; 160 nm for Sn, 120 nm for Cu, and 340 nm for ZnS. We increased both of the thicknesses of Sn and ZnS than those of the precursor of PA120 to optimize the compositions of the resulted CZTS films. Fig. 7 shows the SEM micrograph of the surface of the precursor of Type-PB. By comparing this figure with Fig. 4 of the conventional precursor of Type-PA, it is evident that the surface morphology of precursor of Type-PB is much improved.

Through the sulfurization of the precursors of Type-PB, CZTS thin films, named CZTS-B, were synthesized. The procedure of sulfurization is nearly the same as that of CZTS-A, with the exception of the history of the substrate temperature. For CZTS-B, the substrate temperature was raised up to the final temperature from the room temperature

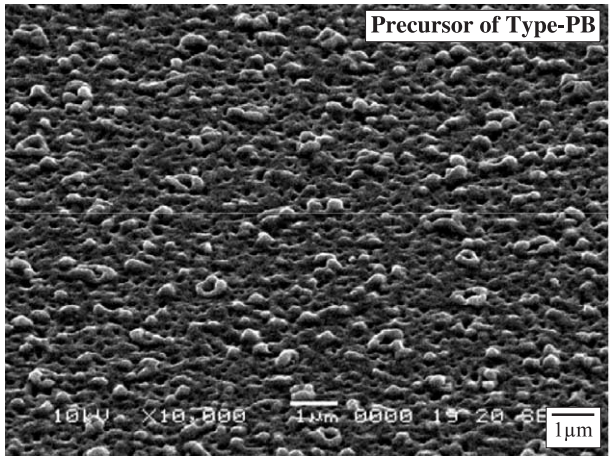


Fig. 7. SEM micrograph of the surface of the precursor of type-PB. This precursor is prepared with new order of Sn/Cu/ZnS.

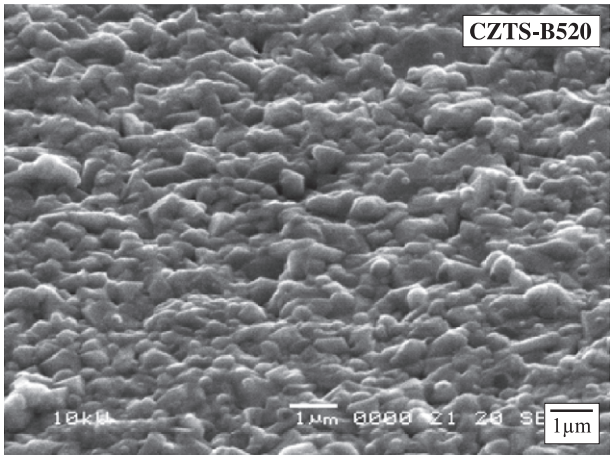


Fig. 8. SEM micrograph of the surface of CZTS film using the precursor of type-PB.

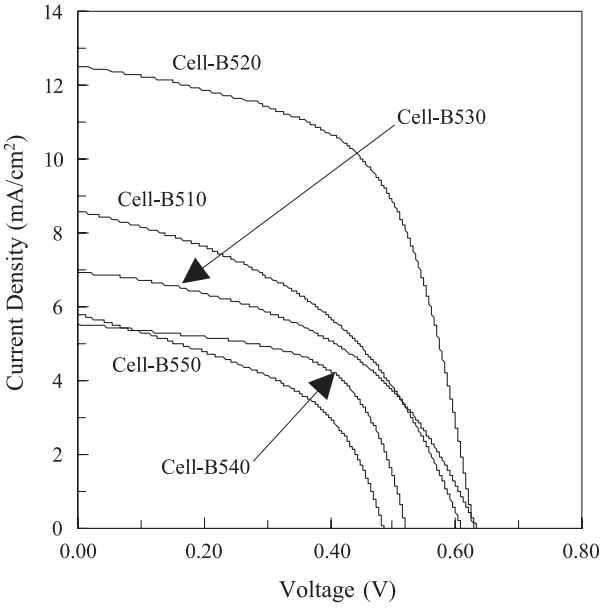


Fig. 9. Illuminated *I–V* characteristics of cells B510 to B550. These numbers correspond to the sulfurization temperature.

at the rate of 5 °C/min. The final temperature was varied from 510 to 550 °C to optimize the sulfurization condition. The final temperature was maintained for 3 h. After the sulfurization, the furnace was cooled naturally to the room temperature. These CZTS films prepared by the sulfurization of precursors of Type-PB were named as CZTS-B510 to B550 corresponding to their final temperatures.

Fig. 8 shows the SEM micrograph of the surface of CZTS-B520. By comparing this figure with Fig. 3 of CZTS-A120, it is confirmed that the grain size of CZTS-B becomes smaller than that of CZTS-A. There are, however, not any large voids at the surface of CZTS-B. Table 4 shows the ratios of the chemical compositions of CZTS-B determined by EDS measurements. Because all the precursors used in this experiment were prepared at the same time, they had the same compositions. We can see no large deviation in the composition in all the films of CZTS-B. Furthermore, we can see the composition ratio is close to the optimized ratio that was mentioned for CZTS-A. Figs. 9 and 10 show the *I–V* characteristics and the quantum efficiency of Cell-B, respectively. Table 5 shows the photovoltaic properties obtained from the *I–V* characteristics. The Cell-B520, of which the sulfurization temperature is 520 °C and the active area is 0.113 $cm^2$, showed the open-circuit voltage of 629 mV, the short-circuit current of 12.53 $mA/cm^2$, the fill factor of 0.58 and the conversion efficiency of 4.53%. The open-circuit voltage decreases with increase in the ratio of Cu/(Zn+Sn), except for Cell-B530. This tendency corresponds to that shown for Cell-A. The dependence of the short-circuit current on the ratio of Zn/Sn, which was shown for Cell-A, was not confirmed for Cell-B. In Fig. 10, we can find that there is no clear degradation of quantum efficiency in the short wavelength region. The degradation was, however, confirmed for Cell-A90 and A100. The configurations of each spectrum are similar except for Cell-B510. The configuration of the quantum efficiency of Cell-B510 is higher than that of the others in the long wavelength region.

Fig. 11 shows the *C–V* characteristics of Cell-B. By extrapolating these plots, we estimated the built-in voltage of Cell-B510 and B520 as 1.1 and 1.5 V, respectively. By using both these built-in voltages and the intersection points on the vertical axis, we estimated the impurity concentration of CZTS-B510 and B520 as $2\times10^{16}$ and $6\times10^{16}$ $cm^{-3}$, respectively. We estimated, in the same way, the impurity concentration of CZTS sulfurized at the temperature of over 530 °C as in the order of $10^{18}$ $cm^{-3}$. In this estimation, according to the relative permittivity of $CuInS_2$ reported as 11 by Shay et al. [9], we used the value of 10 for that of CZTS. In Fig. 10, for the cells of which the impurity concentration were in the order of $10^{18}$ $cm^{-3}$ in the range of the wavelength over 550 nm, the quantum efficiency

Table 4
Chemical compositions of CZTS films of Type-B with various sulfurization temperature

| CZTS name | Temperature (°C) | Chemical compositions (at.%) | | | | Ratio of composition | | |
|---|---|---|---|---|---|---|---|---|
| | | Cu | Zn | Sn | S | Cu/(Zn+Sn) | Zn/Sn | S/Metal |
| CZTS-B510 | 510 | 21 | 12 | 13 | 54 | 0.85 | 0.93 | 1.18 |
| CZTS-B520 | 520 | 21 | 13 | 12 | 53 | 0.85 | 1.03 | 1.18 |
| CZTS-B530 | 530 | 22 | 13 | 12 | 54 | 0.88 | 1.04 | 1.18 |
| CZTS-B540 | 540 | 21 | 13 | 11 | 54 | 0.87 | 1.14 | 1.18 |
| CZTS-B550 | 550 | 21 | 13 | 12 | 54 | 0.88 | 1.09 | 1.18 |

Table 5
Photovoltaic properties of cells of Type-B

| Cell name | Temperature (°C) | Area ($cm^2$) | Voc (mV) | Isc ($mA/cm^2$) | Efficiency (%) | FF | Rs (Ω) | Rsh (Ω) |
|---|---|---|---|---|---|---|---|---|
| Cell-B510 | 510 | 0.101 | 610 | 8.59 | 2.29 | 0.44 | 21.2 | 321 |
| Cell-B520 | 520 | 0.113 | 629 | 12.53 | 4.53 | 0.58 | 8.5 | 428 |
| Cell-B530 | 530 | 0.089 | 633 | 6.96 | 2.05 | 0.47 | 24.5 | 837 |
| Cell-B540 | 540 | 0.092 | 521 | 5.53 | 1.71 | 0.59 | 10.5 | 521 |
| Cell-B550 | 550 | 0.085 | 486 | 5.79 | 1.30 | 0.46 | 13.7 | 207 |

decreases monotonously with increase in the wavelength. On the other hand, for the Cell-B510 and B520, the inclination in the range of the wavelength from 550 to 700 nm is slightly different from that of over 700 nm. In particular, the spectrum for the Cell-B510 shows the good configuration just like a trapezoid. In general, the diffusion length of the carrier increases with decrease in the impurity concentration. For Cell-B510 of which the impurity concentration was relatively low, the relative quantum efficiency in the long wavelength region was elevated because the carrier generated at the region far from the surface could reach to the pn junction. The absolute quantum efficiency of Cell-B510 was, however, lower than that of Cell-B520 in the nearly whole wavelength region. Furthermore, owing to the large series resistance of 21.2 ohm, the resulted conversion efficiency of Cell-B510 was limited to 2.29%.

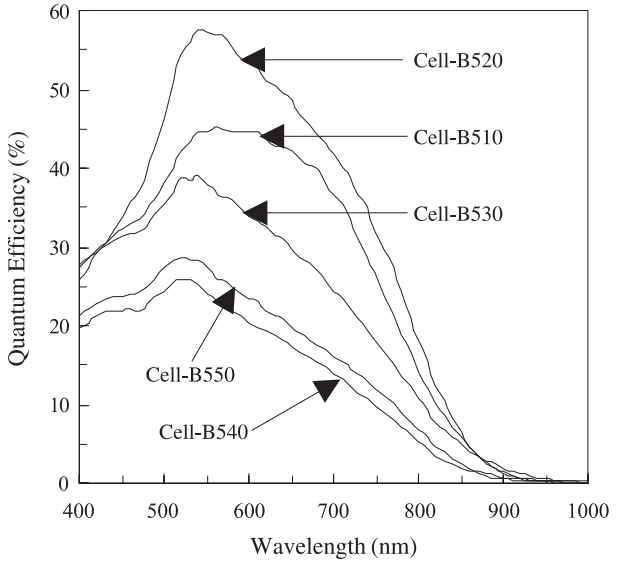


Fig. 10. Quantum efficiency curves of cells B510 to B550.

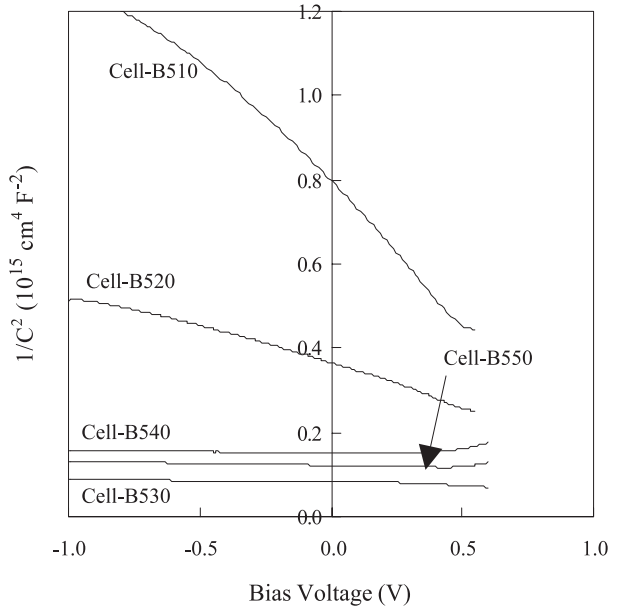


Fig. 11. Relation between $C^{-2}$ and bias voltage of cells B510 to B550.

### 3.3. Multiperiods precursor

Through the experiments mentioned above, it was confirmed that the photovoltaic properties are influenced significantly by the quality of the precursors. We used $SnS_2$ as Sn-source at the stage of precursor fabrication to maintain the surface of the precursor flat as possible and to increase the content of S in them. If we can increase the amount of S in the precursors previously, the volume expansion during the sulfurization period will be able to be suppressed and the resulted adhesion between the film and the substrate will become strong. We fabricated a new type of precursors of 5 periods of $Cu/SnS_2/ZnS$ stacked layers, followed by the annealing in high vacuum to enhance the interdiffusion in the precursor. The thicknesses of layers of each period were as follows: 36 nm for Cu, 88 nm for $SnS_2$, and 66 nm for ZnS. The composition ratios of each element predicted by

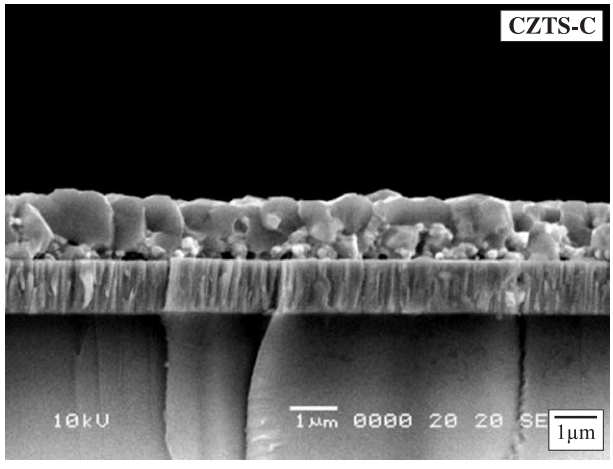


Fig. 12. SEM micrograph of the cross section of CZTS-C on the Mo-coated SLG.

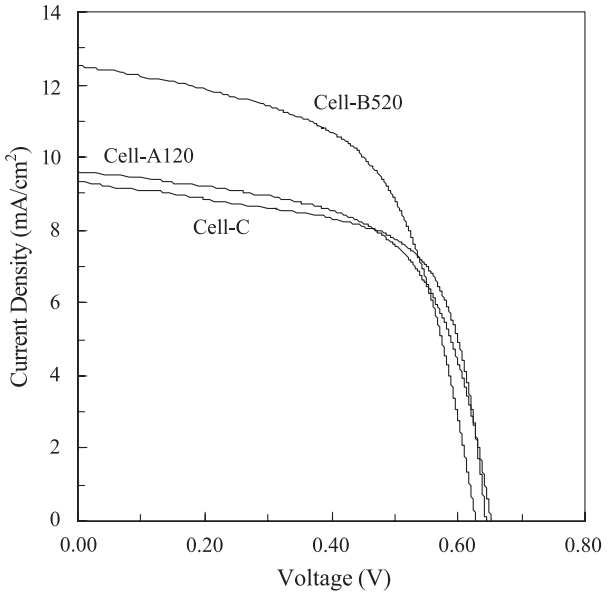


Fig. 13. Comparison of illuminated *I–V* characteristics of CZTS-based solar cells using.

their density and atomic weight were Cu/(Zn+Sn)=1.03 and Zn/Sn=1.28. This precursor, named as PC, was deposited on the heated Mo-coated SLG substrate at the temperature of 200 °C, followed by the annealing with the temperature of 400 °C for 1 h in the same chamber. The sulfurization conditions were slightly modified according to the S-rich composition and the interdiffusion by annealing of the precursor PC. The temperature was raised up to 540 °C at the rate of 10 °C/min. Then, the temperature was maintained at 540 °C for 1 h, followed by the natural cooling to the room temperature.

The composition ratios of the resulted CZTS-C were as follows: Cu/(Zn+Sn)=0.73, Zn/Sn=1.7, and S/Metal=1.1. Fig. 12 shows the SEM micrograph of the cross section of CZTS-C. We obtained some important results; the grain size is as large as the film thickness and the surface is very smooth. By using this CZTS-C as an absorber, Cell-C was produced. For the Cell-C of which the active area is 0.113 $cm^2$, from the result of *I–V* measurement, it was shown that the open-circuit voltage of 644 mV, the short-circuit current of 9.23 $mA/cm^2$, the fill factor of 0.66 and the conversion efficiency of 3.93%. Fig. 13 shows the comparison of the *I–V* characteristics of Cell-A120, B520 and Cell-C. Each open-circuit voltage of these cells shows nearly the same value. Although the short-circuit current of the Cell-C, was the worst value, the fill factor of 0.66 was the best value in this study. This is due to the minimum series resistance of 5.0 ohm in Cell-C. Although the CZTS-C has both Cu-poor and remarkable Zn-rich compositions, the photovoltaic properties were not so degraded. From this result, it was confirmed that the interdiffusion in the precursor is the important factor to attain the higher conversion efficiency of CZTS-based thin film solar cells than those previously developed.

## 4. Conclusions

For the development of the solar cell without environmental contaminants, a new type of a thin film solar cell was fabricated using CZTS film as the absorber. By optimizing the compositions of CZTS absorber, the order of stacked layer in precursor, and the sulfurization condition, the present study could achieve the maximum conversion efficiency of 4.53%. By using the multiperiods precursors that were annealed in high vacuum, the highest fill factor of 0.66 was achieved. Compared with the conventional stacked precursors of the other CZTS films, the surface morphology was much improved in this study. The nontoxic solar cells combining this film with Cd-free buffer layer could be produced because CZTS film does contain neither rare metal nor toxic material. The present study could show the possibility of a very low cost solar cell without any environmental contaminant.

## Acknowledgements

This work was supported in part by a Grant-in-Aid for the development of Scientific Research from the Ministry of Education, Culture, Sports, Science and Technology, Japan (No. 13650022) and by the Incorporated Administrative Agency New Energy and Industrial Technology Development Organization (NEDO) under Ministry of Economy, Trade and Industry (METI), Japan.

## References

[1] J. Emsley, The Elements, 3rd ed., Oxford Univ. Press, Oxford, 1998, p. 289.
[2] K. Ito, T. Nakazawa, Jpn. J. Appl. Phys. 27 (1988) 2094.
[3] K. Ito, T. Nakazawa, Proceedings of the 4th International Conference of Photovoltaic Science and Engineering, Sydney, 1989, p. 341.
[4] Th.M. Friedlmeier, N. Wieser, T. Walter, H. Dittrich, H.-W. Schock, Proceedings of the 14th European Conference of Photovoltaic Science and Engineering and Exhibition, Bedford, 1997, p. 1242.
[5] J.S. Seol, S.Y. Lee, J.C. Lee, H.D. Nam, K.H. Kim, Sol. Energy Mater. Sol. Cells 75 (2003) 155.
[6] H. Katagiri, N. Sasaguchi, S. Hando, S. Hoshino, J. Ohashi, T. Yokota, Technical Digest of the 9th International Conference of Photovoltaic Science and Engineering, Miyazaki, 1996, p. 745.
[7] H. Katagiri, K. Saitoh, T. Washio, H. Shinohara, T. Kurumadani, S. Miyajima, Technical Digest of the 11th International Photovoltaic Science and Engineering Conference, Sapporo, 1999, p. 647.
[8] H. Katagiri, K. Jimbo, K. Moriya, K. Tsuchida, Proceedings of the 3rd World Conference on Photovoltaic Solar Energy Conversion, Osaka, 2003, p. 2874.
[9] J.L. Shay, B. Tell, H.M. Kasper, L.M. Shiavone, Phys. Rev., B 5 (1972) 5003.